AGU PUBLICATIONS

Geophysical Research Letters

RESEARCH LETTER
10.1002/2016GL069453

Key Points:
- SAM-driven rainfall will mitigate the drying of the SH subtropics in summer under RCP8.5
- A poleward expansion of the SH subtropics due to the positive trend in the SAM is a winter phenomenon
- CMIP5 models poorly simulate the observed relationship between the SAM and El Nino-Southern Oscillation

Supporting Information:
- Supporting Information S1

Correspondence to:
E.-P. Lim,
e.lim@bom.gov.au

Citation:
Lim, E.-P., H. H. Hendon, J. M. Arblaster, F. Delage, H. Nguyen, S.-K. Min, and M. C. Wheeler (2016), The impact of the Southern Annular Mode on future changes in Southern Hemisphere rainfall, *Geophys. Res. Lett.*, *43*, 7160–7167, doi:10.1002/2016GL069453.

Received 4 MAY 2016
Accepted 20 JUN 2016
Accepted article online 22 JUN 2016
Published online 9 JUL 2016

The impact of the Southern Annular Mode on future changes in Southern Hemisphere rainfall

Eun-Pa Lim[1], Harry H. Hendon[1], Julie M. Arblaster[2,3], Francois Delage[1], Hanh Nguyen[1], Seung-Ki Min[4], and Matthew C. Wheeler[1]

[1]Bureau of Meteorology, Melbourne, Victoria, Australia, [2]National Center for Atmospheric Research, Boulder, Colorado, USA, [3]School of Earth, Atmosphere & Environment, Monash University, Clayton, Victoria, Australia, [4]School of Environmental Science and Engineering, Pohang University of Science and Technology, Pohang, South Korea

Abstract A robust positive trend in the Southern Annular Mode (SAM) is projected for the end of the 21st century under the Representative Concentration Pathway 8.5 scenario, which results in rainfall decreases in the midlatitudes and increases in the high latitudes in the Southern Hemisphere (SH). We find that this SAM trend also increases rainfall over the SH subtropics in austral summer but not in winter, leading to a pronounced wintertime poleward expansion of the subtropical dry zone. These dynamically driven rainfall changes by the SAM appear to oppose the thermodynamically driven projected rainfall changes in the SH subtropics and midlatitudes, whereas the two components reinforce each other in the high latitudes. However, we show that most climate models fall short in capturing the observed SAM component driven by the El Niño–Southern Oscillation and associated rainfall in the austral warm seasons, which limits our confidence in quantifying the contribution of the SAM to projected rainfall changes.

1. Introduction

The Southern Annular Mode (SAM) is the leading mode of variability of the Southern Hemisphere (SH) extratropical circulation on weekly to centennial time scales [e.g., *Trenberth*, 1979; *Kidson*, 1988; *Hartmann and Lo*, 1998; *Thompson and Wallace*, 2000]. The positive phase of the SAM (positive SAM) is characterized by a poleward shift of the eddy-driven jet that typically sits at ~50°S, resulting in a poleward shift of the SH storm track with concomitant higher surface pressure in the midlatitudes and lower surface pressure at high latitudes [e.g., *Hartmann and Lo*, 1998; *Pezza et al*., 2008]. Consequently, zonally symmetric anomalies of reduced rainfall/higher temperature in the midlatitudes and enhanced rainfall/lower temperature in the high latitudes are observed with positive SAM, and vice versa with negative SAM [e.g., *Silvestri and Vera*, 2003; *Reason and Rouault*, 2005; *Gillett et al*., 2006; *Sen Gupta and England*, 2006; *Hendon et al*., 2007; *Meneghini et al*., 2007]. Furthermore, *Kang et al*. [2011], *Purich et al*. [2013], and *Hendon et al*. [2014a] noted that positive SAM tends to increase rainfall over the SH subtropics in austral spring-summer-autumn by inducing anomalous upward motion in the subtropics, thus acting to shift poleward the descending branch of the Hadley circulation. *Hendon et al*. [2014a] further argued that such change in the poleward extent of the Hadley circulation and associated increase of subtropical rainfall during positive SAM are nearly absent in austral winter due to the presence of the strong winter subtropical jet, which acts as a buffer between variations of the midlatitude to high-latitude circulation and the Hadley circulation in the SH. As a result, the SH subtropical dry zone *shifts* poleward during spring-summer-autumn but *expands* poleward during winter in association with a positive excursion of the SAM.

The SAM is regarded as primarily a stochastic component of weather variability with a typical decorrelation time of ~2 weeks [e.g., *Lorenz and Hartmann*, 2001]. However, its low-frequency variability can be forced by the El Niño–Southern Oscillation (ENSO) [e.g., *Karoly*, 1989], stratospheric polar ozone depletion [e.g., *Thompson and Solomon*, 2002; *Fyfe et al*., 2012; *Arblaster et al*., 2014], and increasing greenhouse gases (GHGs) [e.g., *Fyfe et al*., 1999, 2012]. In particular, a strong positive trend in the SAM is one of the most robust projections of the 21st century climate as a result of increasing GHGs [e.g., *Arblaster and Meehl*, 2006]. Hence, projected changes in future rainfall in the SH subtropics and extratropics will be sensitive to the future behavior of the SAM that will be subject to the strength of GHG forcing relative to that of stratospheric ozone forcing [e.g., *Barnes et al*., 2014, *Zheng et al*., 2014; *Wang et al*., 2014] and also to the response of ENSO to the GHG forcing [e.g., *Yeh et al*., 2009; *Vecchi and Wittenberg*, 2010].

The current study is aimed at investigating the contribution of the projected robust changes in the SAM to the changes of SH precipitation at the end of the 21st century with focus on its seasonality. For this study,

we use the models submitted to Phase Five of the Coupled Model Intercomparison Project (CMIP5) with the radiative forcing following the Representative Concentration Pathway 8.5 (RCP8.5) [e.g., *Flato et al*., 2013]. The end of the 21st century with the RCP8.5 scenario is considered here because a strong positive trend is projected for the SAM as a result of the GHGs being a dominant forcing [e.g., *Zheng et al*., 2014], and therefore, a clear influence of the SAM on future rainfall changes can be identified. We will first examine the capability of the CMIP5 models to simulate the observed relationship between SH rainfall variations and the SAM in contrasting summer (December–February; DJF) and winter (June–August; JJA) seasons by comparing relationships in the historical simulations of the CMIP5 to observed behavior for the base period of 1979–2005. Then, we will diagnose the role of the projected changes in the SAM for the changes in rainfall for 2071–2100 with the RCP8.5 scenario.

2. Models and Data

We analyze the historical runs for the period 1979–2005, for which high-quality global reanalysis data sets are available, and the RCP8.5 scenario runs for the period 2006–2100, using 37 models (one simulation per model) of the CMIP5 [*Flato et al*., 2013] (Table S1 in the supporting information). The model outputs are interpolated to 1.5° latitude by 1.5° longitude grids.

The SAM index is formed by the difference of normalized 3 month averaged mean sea level pressure (MSLP) anomalies at 40°S and 65°S, following the definition of *Gong and Wang* [1999]. The modeled SAM and rainfall from the historical runs of the CMIP5 are compared to the observed SAM diagnosed using MSLP from the ERA-Interim reanalyses [*Dee et al*., 2011] and the monthly GPCP rainfall analyses [*Adler et al*., 2003], respectively, for the period 1979–2005. The GPCP rainfall data set is chosen for this study because it incorporates surface rain gauge observations as well as satellite observations, and therefore, it would provide reliable estimate of rainfall response to the SAM especially over the SH continents [e.g., *Hendon et al*., 2014a].

A significant proportion of SAM variation is observed to be forced by ENSO in austral warm seasons but not in austral cold seasons [e.g., *Karoly*, 1989; *L'Heureux and Thompson*, 2006; *Lim et al*., 2013; *Wang and Cai*, 2013]. Therefore, we examine the CMIP5 models' ability to simulate the seasonality of this teleconnection by correlating the SAM index with the Niño 3.4 index defined by the sea surface temperature (SST) anomalies averaged over 5°S–5°N, 120°W–170°W. The observed Niño 3.4 index is computed, using *Hurrell et al*.'s [2008] SST analyses. Lastly, all anomalies are computed relative to the base period 1979–2005.

3. Observed Relationship of SH Rainfall and the SAM

Based on observations for the period 1979–2005, positive SAM is associated with nearly zonally uniform increases of rainfall in the SH high latitudes and decreases of rainfall in the SH midlatitudes in all seasons [e.g., *Gillett et al*., 2006; *Sen Gupta and England*, 2006; *Hendon et al*., 2014a] (Figures 1a and 1b). However, the rainfall relationship with the SAM (both increase and decrease) over the subtropics (equatorward of 30°S) is stronger in summer than in winter, which appears to be largely due to the covariability of the SAM and ENSO in austral warm seasons (Figure 1c) [e.g., *Hendon et al*., 2014a]. When further removing the influence of the SAM trend from the ENSO-independent SAM and rainfall relationship (cf. Figures 1e and 1c), there is little change compared to removing ENSO only from the original SAM index (cf. Figures 1c and 1a). Once the ENSO signal and the trend are regressed out from the SAM index, the overall strength of the relationship between SAM and rainfall is comparable between summer and winter over the SH subtropics and extratropics (Figures 1c–1f).

A close inspection of the rainfall regression to the ENSO-removed detrended SAM (Figures 1e and 1f) reveals that the zonally symmetric dry zone associated with positive SAM in the midlatitudes starts slightly more poleward in summer than in winter (Figures 1e and 1f, dashed red lines; also see Figure S1 in the supporting information). Furthermore, a substantial increase in rainfall is observed over South Africa and Australia, southern Brazil, and the southern part of the South Pacific Convergence Zone (SPCZ) during positive SAM in summer, which is not seen in winter except for over eastern Australia and southern Brazil. These features are found even with an extended analysis period of 1979–2014 and with the use of *Marshall*'s [2003] SAM index (except for the winter rainfall response over the tropical Pacific region and across inland Australia being somewhat different with *Marshall*'s [2003] SAM index but without statistical significance; not shown).

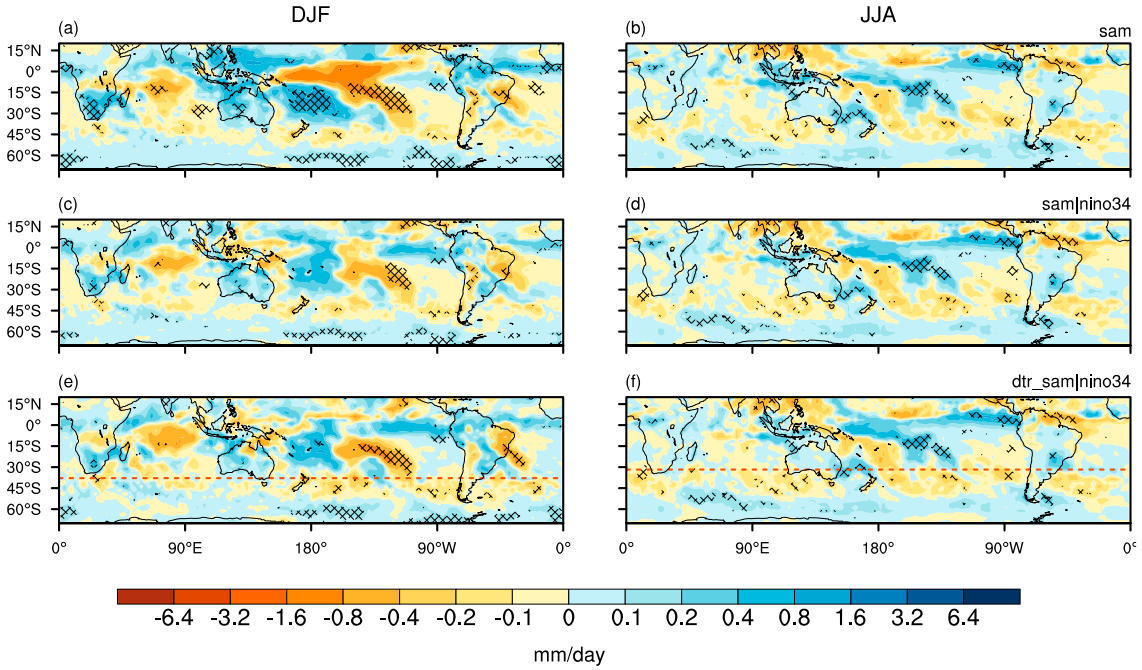

Figure 1. Regression of GPCP rainfall to (a and b) the SAM index, (c and d) the ENSO-removed SAM index, and (e and f) the ENSO-removed and detrended SAM index in December-January-February (DJF; Figures 1a, 1c, and 1e) and June-July-August (JJA; Figures 1b, 1d, and 1f) over 1979–2005. The dashed red line in Figures 1e and 1f indicates the latitude where zonal mean rainfall regression to the SAM changes its sign between the SH subtropics and the SH midlatitudes as shown in Figure S1 (i.e., the latitude where the SAM-driven midlatitude dry zone starts). Hatching indicates statistically significant regression at the 90% confidence level (c.l.) with 25 degrees of freedom, using a two-tailed Student's *t* test.

This seasonality of the impact of the SAM on subtropical rainfall is consistent with the findings of *Hendon et al.* [2014a]. They argued that the absence of the distinctive subtropical jet in summer leads to a meridionally narrower subtropical breaking zone of extratropical baroclinic eddies during positive SAM, which sets a steeper than normal latitudinal gradient of eddy-driven southward flow. The associated stronger divergence of meridional flow induces stronger upward motion and associated rainfall increase in the SH subtropics in summer during positive SAM. For the same reason, *Hendon et al.* [2014a] attributed the equatorward expanded midlatitude dry conditions and the lack of subtropical rainfall response during positive SAM in winter to the presence of the strong subtropical jet.

4. The SAM-Rainfall Relationship in the CMIP5 Historical Simulations

At first glance, the observed SAM-rainfall relationship is well reproduced in the CMIP5 historical runs (CMIP5 HIST) (Figures 2 and S1). This includes the shift to wetter subtropics-drier midlatitudes-wetter high latitudes in summer and the northward expanded drier midlatitudes-wetter high latitudes in winter associated with positive SAM. However, while the strength of the observed relationship between the SAM and subtropical rainfall is sensitive to the SAM-ENSO connection in summer, such sensitivity is hardly reproduced in the CMIP5 HIST (Figures 2a and 2c compared to Figures 1a and 1c). This lack of sensitivity is because most of the models fall significantly short in simulating the seasonality of the correlation between the SAM and ENSO (Figure 3a). Only bcc-csm1-1-m and CMCC-CM skilfully simulate the seasonality of the SAM-ENSO connection with maximum negative correlations in the warm seasons and minimum correlations in the cold seasons. The SAM trend in the warm seasons is also significantly underestimated in these historical run as reported in *Zheng et al.* [2014] (Figure 3b). The seasonality and magnitude of the observed SAM trend is only captured in five models (bcc-csm1-1-m, CMCC-CESM, HadGEM2-AO, IPSL-CM5B-LR, and MPI-ESM-MR).

Although the majority of the models fail to simulate these two key forced components of SAM variation, the models skillfully reproduce the relationship between the internally driven SAM and the rainfall in both summer and winter (Figures 2e and 2f). The poleward shift of the northern boundary of the rainfall decrease and the increase of the subtropical rainfall over South Africa, Australia, and the southern part of SPCZ during

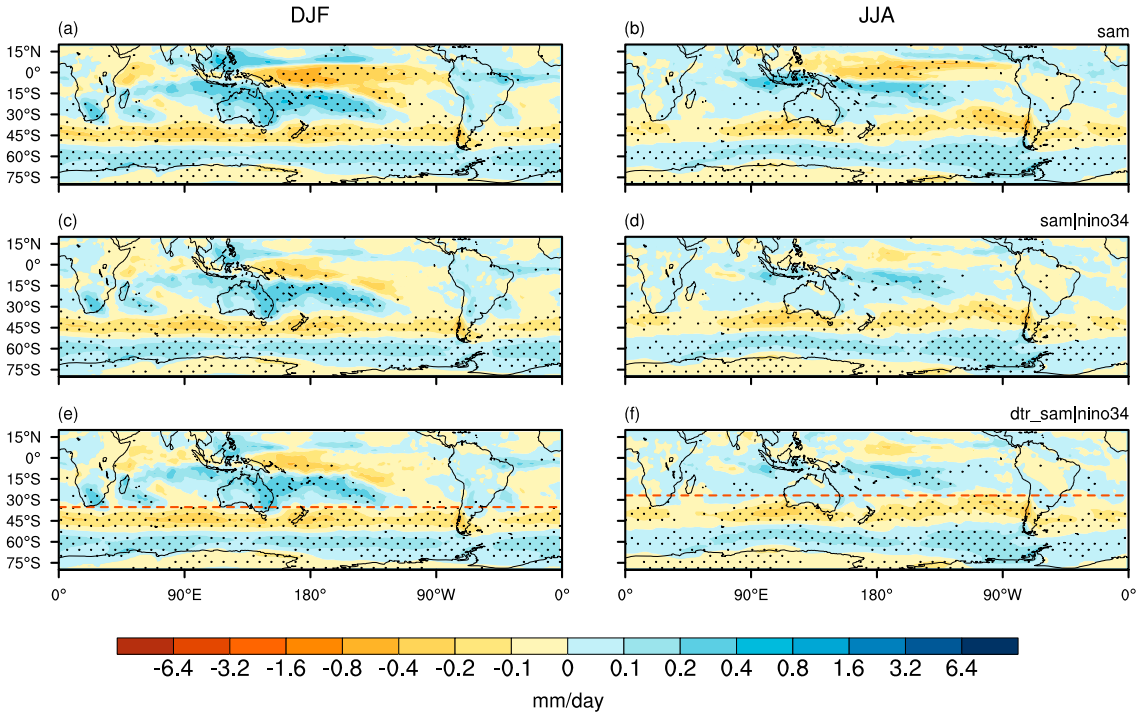

Figure 2. The same as Figure 1 but the mean of the rainfall regressions to the SAM of the 37 models in the CMIP5 HIST. Stippling indicates where three quarters or more of the models agree with the mean of the regressions (i.e., the multimodel mean) between the rainfall and the SAM. The dashed red line in Figures 2e and 2f indicates the latitude where the mean of individual model zonal mean rainfall regression to the SAM changes its sign between the SH subtropics and the SH midlatitudes (Figure S1).

positive SAM in summer as compared to winter are correctly simulated. The good match between the observed and the mean of the models for the rainfall relationship with the internally driven SAM in both seasons is confirmed in the regression pattern of the zonal mean rainfall onto the SAM, as shown in Figure S1. In contrast, the sign of the SAM-driven rainfall change in the models is opposite to that in the observation over the subtropical central Pacific and northern Chile in summer, and the models significantly overestimate the SAM-driven dry conditions over the southern parts of Chile and Argentina in winter (Figure 2).

Notwithstanding the relatively poor simulation of the ENSO-SAM relationship and SAM trend and the misrepresentation of some local relations of the SAM-rainfall, the models skilfully capture the overall pattern and strength of the SH rainfall relation to the internally driven SAM and its seasonality. Hence, we will explore the

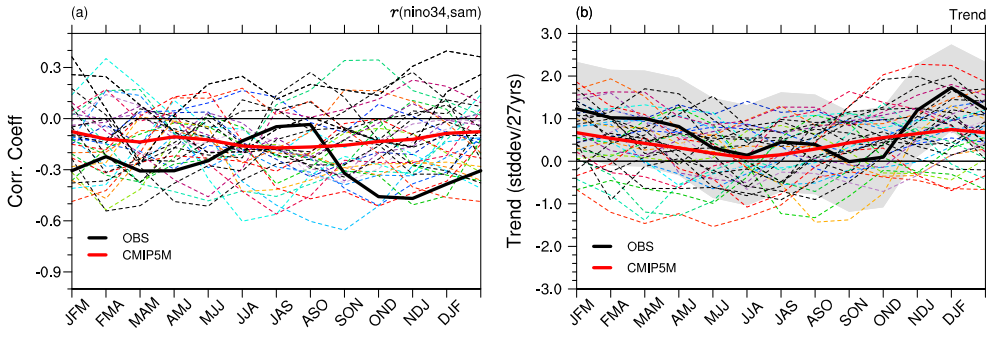

Figure 3. (a) Correlation of the SAM and Niño3.4 SST indices and (b) the trend of the SAM index over the 1979–2005 for the observation (black solid curve) and the CMIP5 HIST (thin dotted curves for individual models and red solid curve for the mean of individual model correlations and regressions (i.e., the multimodel mean)). Correlation coefficients greater than 0.33 are statistically significant at the 90% c.l. with 27 independent samples, using a two-tailed Student's *t* test in Figure 3a, and the 90% confidence interval for the observed trend is shown with the grey shading in Figure 3b.

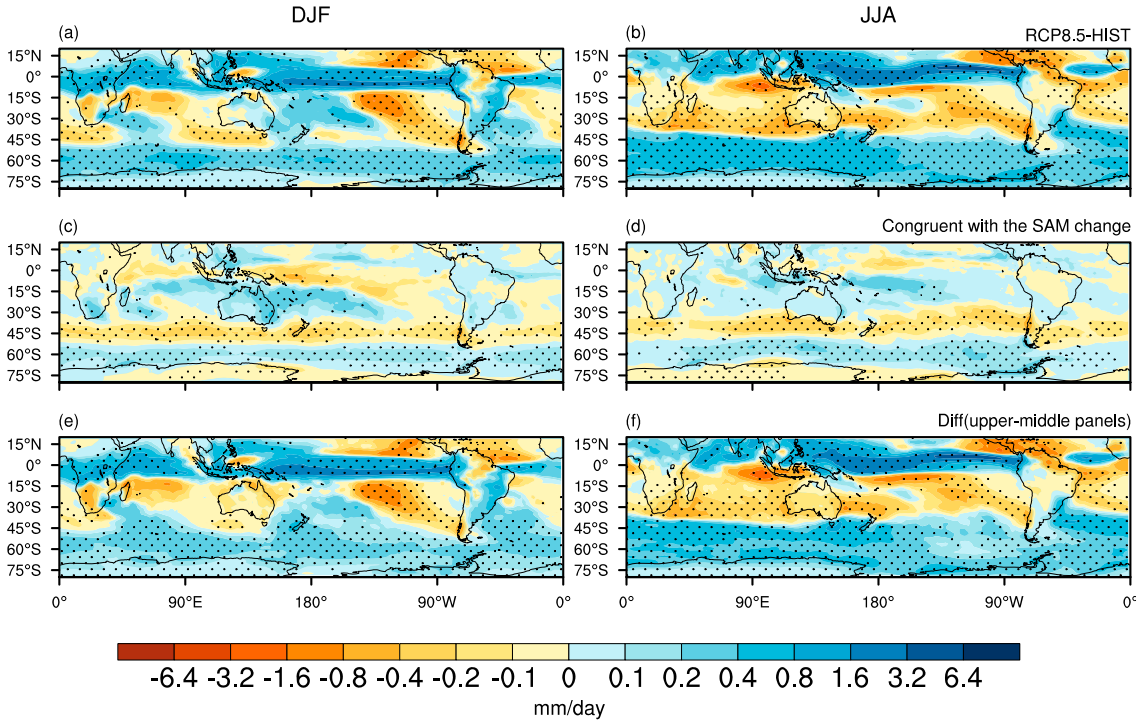

Figure 4. Rainfall changes (a, b) 2071–2100 from the CMIP5 RCP8.5 compared to 1979–2005 from the CMIP HIST; (c, d) as in Figures 4a and 4b but congruent with the SAM change; and (e, f) the difference between Figures 4a and 4b and 4c and 4d. Stippling indicates where three quarters or more of the models agree with the multimodel mean changes.

proportion of the projected rainfall change in the last 30 years of the 21st century resulting from the upward trend in the SAM.

5. Projected Changes in SH Rainfall by the End of the 21st Century

Projected rainfall changes obtained from the last 30 years (2071–2100) of the CMIP5 RCP8.5 compared to the 27 years (1979–2005) of the CMIP5 HIST demonstrate strong increases of rainfall in the tropics and the SH mid-high latitudes and decreases in the SH subtropics (Figures 4a and 4b) [see also, e.g., *Collins et al.*, 2013]. It is interesting to note that the wet-dry-wet pattern of the change from the tropics to the SH extratropics is much more pronounced in winter than in summer, with projected significant drying over South Africa, southern Madagascar, eastern and western Australia, and central Chile.

We now address how much of these projected rainfall changes stems from the projected trend in the SAM. We base the analysis on the SAM index that is linearly independent of ENSO (hereafter, $SAM_{|enso}$). Because the weak relation of the SAM and ENSO shown in the mean of the CMIP5 HIST simulations stays unchanged throughout the 21st century in the CMIP5 RCP8.5 (not shown), the removal of the ENSO from the SAM index does not make a significant difference in the results presented in the rest of the paper. An upward trend in the $SAM_{|enso}$ is robustly projected to result from increasing GHGs [e.g., *Kushner et al.*, 2001; *Cai et al.*, 2003; *Miller et al.*, 2006; *Gillett and Fyfe*, 2013; *Purich et al.*, 2013; *Zheng et al.*, 2014] (Figure S2). Using the RCP8.5 scenario, a positive trend in the $SAM_{|enso}$ is found in all seasons with the largest trend (~2 standard deviation (σ) increase over 1979–2100) in autumn from April to June and the smallest trend (~1.3σ) in summer from November to February (Figure S3). The smallest positive trend in the SAM in summer is likely to result from the competing effects between the recovery of the Antarctic stratospheric ozone and the increasing GHGs in the first half of the 21st century as suggested by *Barnes et al.* [2014] and *Wang et al.* [2014].

To estimate the change in rainfall that is congruent with the change of the $SAM_{|enso}$, we scale the regression coefficients, which were obtained by regressing the rainfall anomalies onto the detrended $SAM_{|enso}$ index using the CMIP5 HIST for the 1979–2005 period (Figures 2e and 2f), by the difference of the $SAM_{|enso}$ index from 1979–2005 to 2071–2100. We can justify the use of this method as the relationship between rainfall

anomalies and the detrended $SAM_{|enso}$ remains relatively unchanged in the 21st century simulations (Figure S4). The regression coefficients and the $SAM_{|enso}$ index are calculated in each of 37 models, and the multimodel mean of the individual scaled regressions is shown in Figures 4c and 4d. The multimodel mean change of the $SAM_{|enso}$ between the two periods is 1.0σ in summer and 1.4σ in winter. As expected from the SAM-rainfall association simulated in the CMIP5 HIST, the projected positive trend of the $SAM_{|enso}$ appears to result in significant increases of the rainfall over the SH subtropics including South Africa and Australia; significant decreases of the rainfall over the SH midlatitudes including Tasmania of Australia, New Zealand, and the southern tips of Chile and Argentina; and significant increases of the rainfall over the Antarctic circumpolar trough region in summer (Figure 4c).

Overall, a similar pattern of rainfall change associated with the $SAM_{|enso}$ is found in winter (Figure 4d). However, in winter the northern boundary of the midlatitude drying signal associated with the $SAM_{|enso}$ is extended equatorward reaching the southern ends of the Australian continent, and the $SAM_{|enso}$-congruent increase of the subtropical rainfall is not as strong as in summer. These two winter features of the $SAM_{|enso}$-rainfall relationship together explain how the positive trend of the SAM would contribute to the poleward expansion of the SH subtropical dry zone in the future climate with increasing GHGs [e.g., *Previdi and Liepert*, 2007]. A significant rainfall reduction associated with the positive trend of the $SAM_{|enso}$ is seen over the southern tip of South America in winter, but there is a large uncertainty in this winter change due to the low skill of the models to reproduce the observed South American rainfall-SAM relationship in the CMIP5 HIST as shown in Figures 2b, 2d, and 2f.

A comparison of the total projected rainfall changes to those congruent with the $SAM_{|enso}$ change reveals that the projected rainfall changes tend to be offset by the rainfall changes driven by the enhanced positive $SAM_{|enso}$ in the SH subtropics (equatorward of ~30°S) and midlatitudes (~30°–50°S) in summer and in the SH midlatitudes (~40°–50°S) in winter (Figures 4c–4f). In other words, the positive trend of the $SAM_{|enso}$ appears to play a mitigating role for the drying of the SH subtropics and the wettening of the SH midlatitudes projected in the end of the 21st century. Previous studies [e.g., *Emori and Brown*, 2005; *Held and Soden*, 2006; *Seager et al*., 2010] have shown that an increase of the atmospheric moisture content in a warmer world, following the Clausius-Clapeyron relation (namely, the wet get wetter-dry get drier/thermodynamic processes), is a dominant contributor to the drying of the poleward side of the SH subtropics and the moistening of the SH extratropics. Our investigation with a subset of CMIP5 models (27 models) shows an offset between the SAM-driven and the thermodynamically driven rainfall changes in the SH subtropics and midlatitudes (Figure S5). On the other hand, the strong positive trend in the $SAM_{|enso}$ appears to exacerbate the drying of the southern ends of Australia in winter (i.e., a poleward expansion of the subtropical dry zone) and enhance the significant wettening of the SH polar region in both summer and winter [e.g., *Watterson*, 1998; *Seager et al*., 2010].

6. Concluding Remarks

The SAM is the leading mode of variability of the SH extratropical circulation on various time scales beyond 1 week, and therefore, it significantly impacts the weather and climate of the SH. Given a strong consensus in the climate models that the SAM will trend toward its positive phase in the climate under a scenario of high emissions of GHGs [e.g., *Christensen et al*., 2013; *Zheng et al*., 2014], we have attempted to understand the impact of such change in the SAM on future rainfall by assessing the CMIP5 historical simulations and projected simulations with the RCP8.5 forcing.

Using 37 models from the CMIP5 archive, our analyses show that the historical runs skilfully simulate the observed relationship between the SAM and the SH rainfall in austral summer and winter seasons, although they fall short in capturing the SAM component forced by ENSO and the upward trend in the SAM due to stratospheric SH polar ozone depletion and increasing GHGs. In the last 30 years of the 21st century under the RCP8.5 scenario, the SAM component that is independent of ENSO is projected to be more positive by 1.0σ and 1.4σ than that of the last 27 years of the twentieth century in summer and winter, respectively. These changes of the SAM lead to decreased rainfall in the SH midlatitudes and increased rainfall in the SH high latitudes in both summer and winter. On the other hand, the impact of the future changes of the SAM on SH subtropical rainfall shows strong seasonality with increasing rainfall in summer but not in winter, resulting in a poleward expansion of the subtropical dry zone in the winter season. In comparison, SH rainfall without the contribution of the SAM is projected to decrease in the subtropics and increase in the mid-high

latitudes, a significant portion of which is accounted for by the Clausius-Clapeyron effect. Consequently, projected changes in the SAM appear to mitigate the wettening of the midlatitudes and to enhance the wettening of the Antarctic circumpolar trough region in both summer and winter seasons, while mitigating the drying of the SH subtropics in summer but expanding it poleward in winter.

The teleconnection between the SAM and SH rainfall is observed to be substantially strengthened by the relationship of the SAM with ENSO in the austral warm seasons, which is not captured in the historical runs by most models. The inability of the CMIP5 models to capture the covariability of the SAM and ENSO and associated rainfall substantially limits the confidence in their future rainfall projections, especially regarding the future projections of extreme seasonal rainfall, since it can result from the concurrence of SAM and ENSO events [e.g., *Hendon et al*., 2014b; *Lim and Hendon*, 2015; *Lim et al*., 2016]. Therefore, future research should be prioritized to diagnose the causes of the model bias in simulating this tropical-extratropical interaction and to reduce the bias.

Acknowledgments

This study is supported by the Victorian Climate Initiative. Julie Arblaster is partially supported by the Australian Climate Change Science Program and the Regional and Global Climate Modeling Program (RGCM) of the U.S. Department of Energy's Office of Biological and Environmental Research (BER) Cooperative Agreement DE-FC02-97ER62402. We are grateful to Christine Chung and Scott Power at the Bureau of Meteorology for providing valuable comments on earlier versions of the manuscript. The NCAR Command Language (NCL; NCL 2014) was used for data analysis and visualization of the results. We acknowledge the World Climate Research Programme's Working Group on Coupled Modelling, which is responsible for CMIP, and we thank the climate modeling groups (listed in Table S1 in the supporting information of this paper) for producing and making available their model output. We also acknowledge NCAR/UCAR, ECMWF, and NOAA for producing and providing *Hurrell et al*. [2008] SST analysis, ERA-Interim reanalysis, and GPCP precipitation data.

References

Adler, R. F., et al. (2003), The version-2 Global Precipitation Climatology Project (GPCP) monthly precipitation analysis (1979–present), *J. Hydrometeorol.*, *4*, 1147–1167.

Arblaster, J. M., and G. A. Meehl (2006), Contributions of external forcings to Southern Annular Mode trends, *J. Clim.*, *19*, 2896–2905.

Arblaster, J. M., N. P. Gillett, N. Calvo, P. M. Forster, L. M. Polvani, S.-W. Son, D. W. Waugh, and P. J. Young (2014), Stratospheric ozone changes and climate, in *Scientific Assessment of Ozone Depletion: 2014*, *Global Ozone Research and Monitoring Project – Report No. 55*, Chap. 4, World Meteorol. Organ., Geneva, Switzerland.

Barnes, E. A., N. W. Barnes, and L. M. Polvani (2014), Delayed Southern Hemisphere climate change induced by stratospheric ozone recovery, as projected by the CMIP5 models, *J. Clim.*, *27*(2), 852–867, doi:10.1175/JCLI-D-13-00246.1.

Cai, W., P. H. Whetton, and D. J. Karoly (2003), The response of the Antarctic Oscillation to increasing and stabilized atmospheric CO_2, *J. Clim.*, *16*, 1525–1538.

Christensen, J. H., et al. (2013), Climate phenomena and their relevance for future regional climate change, in *Climate Change 2013: The Physical Science Basis. Contribution of Working Group I to the Fifth Assessment Report of the Intergovernmental Panel on Climate Change*, edited by T. F. Stocker et al., Cambridge Univ. Press, Cambridge, U. K., and New York, doi:10.1017/CBO9781107415324.024.

Collins, M., et al. (2013), Long-term climate change: Projections, commitments and irreversibility, in *Climate Change 2013: The Physical Science Basis. Contribution of Working Group I to the Fifth Assessment Report of the Intergovernmental Panel on Climate Change*, edited by T. F. Stocker et al., Cambridge Univ. Press, Cambridge, U. K., and New York, doi:10.1017/CBO9781107415324.024.

Dee, D. P., et al. (2011), The ERA-Interim reanalysis: Configuration and performance of the data assimilation system, *Q. J. R. Meteorol. Soc.*, *137*, 553–597, doi:10.1002/qj.828.

Emori, S., and S. J. Brown (2005), Dynamic and thermodynamic changes in mean and extreme precipitation under changed climate, *Geophy. Res. Lett.*, *32*, L17706, doi:10.1029/2005GL023272.

Flato, G., et al. (2013), Evaluation of climate models, in *Climate Change 2013: The Physical Science Basis. Contribution of Working Group I to the Fifth Assessment Report of the Intergovernmental Panel on Climate Change*, edited by T. F. Stocker et al., Cambridge Univ. Press, Cambridge, U. K., and New York.

Fyfe, J. C., G. J. Boer, and G. M. Flato (1999), The Arctic and Antarctic Oscillations and their projected changes under global warming, *Geophys. Res. Lett.*, *26*, 1601–1604, doi:10.1029/1999GL900317.

Fyfe, J. C., N. P. Gillett, and G. J. Marshall (2012), Human influence on extratropical Southern Hemisphere summer precipitation, *Geophys. Res. Lett.*, *39*, L23711, doi:10.1029/2012GL054199.

Gillett, N. P., and J. C. Fyfe (2013), Annular mode changes in the CMIP5 simulations, *Geophys. Res. Lett.*, *40*, 1189–1193, doi:10.1002/grl.50249.

Gillett, N. P., T. D. Kell, and P. D. Jones (2006), Regional climate impacts of the Southern Annular Mode, *Geophys. Res. Lett.*, *33*, L23704, doi:10.1029/2006GL027721.

Gong, D., and S. Wang (1999), Definition of Antarctic Oscillation index, *Geophys. Res. Lett.*, *26*(4), 459–462, doi:10.1029/1999GL900003.

Hartmann, D. L., and F. Lo (1998), Wave-driven zonal flow vacillation in the Southern Hemisphere, *J. Atmos. Sci.*, *55*, 1303–1315.

Held, I. M., and B. J. Soden (2006), Robust responses of the hydrological cycle to global warming, *J. Clim.*, *19*, 5686–5699.

Hendon, H. H., D. W. J. Thompson, and M. C. Wheeler (2007), Australian rainfall and surface temperature variations associated with the Southern Hemisphere annular mode, *J. Clim.*, *20*, 2452–2467.

Hendon, H. H., E.-P. Lim, and H. Ngyuen (2014a), Variations of subtropical precipitation and circulation associated with the Southern Annular Mode, *J. Clim.*, *27*, 3446–3460.

Hendon, H. H., E.-P. Lim, J. Arblaster, and D. T. L. Anderson (2014b), Causes and predictability of the record wet spring over Australia in 2010, *Clim. Dyn.*, *42*, 1155–1174, doi:10.1007/s00382-013-1700-5.

Hurrell, J. W., J. J. Hack, D. Shea, J. M. Caron, and J. Rosinski (2008), A new sea surface temperature and sea ice boundary data set for the Community Atmosphere Model, *J. Clim.*, *21*, 5145–5153, doi:10.1175/2008JCLI2292.1.1.

Kang, S., L. M. Polvani, J. C. Fyfe, and M. Sigmond (2011), Impact of polar ozone depletion on subtropical precipitation, *Science*, *332*, 951–954.

Karoly, D. J. (1989), Southern Hemisphere circulation features associated with El Niño-Southern Oscillation events, *J. Clim.*, *2*, 1239–1252.

Kidson, J. W. (1988), Indices of the Southern Hemisphere zonal wind, *J. Clim.*, *1*, 183–194.

Kushner, P. J., I. M. Held, and T. L. Delworth (2001), Southern Hemisphere atmospheric circulation response to global warming, *J. Clim.*, *14*, 2238–2249.

L'Heureux, M. L., and D. W. J. Thompson (2006), Observed relationships between the El Niño–Southern Oscillation and the extratropical zonal-mean circulation, *J. Clim.*, *19*, 276–287.

Lim, E.-P., and H. H. Hendon (2015), Understanding the contrast of Australian springtime rainfall of 1997 and 2002 in the frame of two flavors of El Niño, *J. Clim.*, *28*, 2804–2822.

Lim, E.-P., H. H. Hendon, and H. Rashid (2013), Seasonal predictability of the Southern Annular Mode due to its association with ENSO, *J. Clim.*, *26*, 8037–8054.

Lim, E.-P., H. H. Hendon, J. M. Arblaster, C. Chung, A. F. Moise, P. Hope, G. Young, and M. Zhao (2016), Interaction of the recent 50 year SST trend and La Niña 2010: Amplification of the Southern Annular Mode and Australian springtime rainfall, *Clim. Dyn.*, doi:10.1007/s00382-015-2963-9.

Lorenz, D. J., and D. L. Hartmann (2001), Eddy-zonal flow feedback in the Southern Hemisphere, *J. Atmos. Sci.*, *58*, 3312–3327.

Marshall, G. J. (2003), Trends in the Southern Annular Mode from observations and reanalyses, *J. Clim.*, *16*, 4134–4143.

Meneghini, B., I. Simmonds, and I. Smith (2007), Association between Australian rainfall and the Southern Annular Mode, *Int. J. Climatol.*, *27*, 109–121.

Miller, R. L., G. A. Schmidt, and D. T. Shindell (2006), Forced annular variations in the 20th century Intergovernmental Panel on Climate Change Fourth Assessment Report models, *J. Geophys. Res.*, *111*, D18101, doi:10.1029/2005JD006323.

Pezza, A. B., T. Durrant, and I. Simmonds (2008), Southern Hemisphere synoptic behavior in extreme phases of SAM, ENSO, sea ice extent, and Southern Australia rainfall, *J. Clim.*, *21*, 5566–5584, doi:10.1175/2008JCLI2128.1.

Previdi, M., and B. G. Liepert (2007), Annular modes and Hadley cell expansion under global warming, *Geophys. Res. Lett.*, *34*, L22701, doi:10.1029/2007GL031243.

Purich, A., T. Cowan, S.-K. Min, and W. Cai (2013), Autumn precipitation trends over Southern Hemisphere midlatitudes as simulated by CMIP5 models, *J. Clim.*, *26*(21), 8341–8356, doi:10.1175/JCLI-D-13-00007.1.

Reason, C. J. C., and M. Rouault (2005), Links between the Antarctic Oscillation and winter rainfall over western South Africa, *Geophys. Res. Lett.*, *32*, L07705, doi:10.1029/2005GL022419.

Seager, R., N. Naik, and G. A. Vecchi (2010), Thermodynamic and dynamic mechanisms for large-scale changes in the hydrological cycle in response to global warming, *J. Clim.*, *23*, 4651–4668.

Sen Gupta, A., and M. H. England (2006), Coupled ocean–atmosphere–ice response to variations in the Southern Annular Mode, *J. Clim.*, *19*, 4457–4486.

Silvestri, G. E., and C. S. Vera (2003), Antarctic Oscillation signal on precipitation anomalies over southeastern South America, *Geophys. Res. Lett.*, *30*(21), 2155, doi:10.1029/2003GL018277.

Thompson, D. W. J., and S. Solomon (2002), Interpretation of recent Southern Hemisphere climate change, *Science*, *296*, 895–899.

Thompson, D. W. J., and J. M. Wallace (2000), Annular modes in the extratropical circulation. Part I: Month-to-month variability, *J. Clim.*, *13*, 1000–1016.

Trenberth, K. E. (1979), Interannual variability of the 500 mb zonal flow in the Southern Hemisphere, *Mon. Weather Rev.*, *107*, 1515–1524.

Vecchi, G. A., and A. T. Wittenberg (2010), El Niño and our future climate: Where do we stand? *Wiley Interdiscip. Rev. Clim. Change*, *1*(2), doi:10.1002/wcc.33.

Wang, G., and W. Cai (2013), Climate-change impact on the 20th-century relationship between the Southern Annular Mode and global mean temperature, *Sci. Rep.*, *3*, 3133–3136, doi:10.1038/srep02039.

Wang, G., W. Cai, and A. Purich (2014), Trends in Southern Hemisphere wind-driven circulation in CMIP5 models over the 21st century: Ozone recovery versus greenhouse forcing, *J. Geophys. Res. Oceans*, *119*, 2974–2986, doi:10.1002/2013JC009589.

Watterson, I. G. (1998), An analysis of the global water cycle of present and doubled CO_2 climates simulated by the CSIRO general circulation model, *J. Geophys. Res.*, *103*, 23,113–23,129, doi:10.1029/98JD02022.

Yeh, S.-W., J.-S. Kug, B. Dewitte, M.-H. Kwon, B. P. Kirtman, and F.-F. Jin (2009), El Niño in a changing climate, *Nature*, *461*(7263), 511–514, doi:10.1038/nature08316.

Zheng, F., J. Li, R. T. Clark, and H. C. Nnamchi (2014), Simulation and projection of the Southern Hemisphere annular mode in CMIP5 models, *J. Clim.*, *26*, 9860–9879.